Photo Reactions in Few-Body Systems - From Nuclei to Cold-Atoms

Nir Barnea

The Racah institute for Physics
The Hebrew University, Jerusalem, Israel

TRIUMF
14 September 2012

האוניברסיטה העברית בירושלים
The Hebrew University of Jerusalem

Collaboration

Jerusalem, Israel
B. Bazak*, D. Gazit, E. Liverts, N. Nevo*

Trento, Italy
W. Leidemann, G. Orlandini

Moscow, Russia
V. Efros

TRIUMF, Canada
S. Bacca

What can we learn from photo reactions?

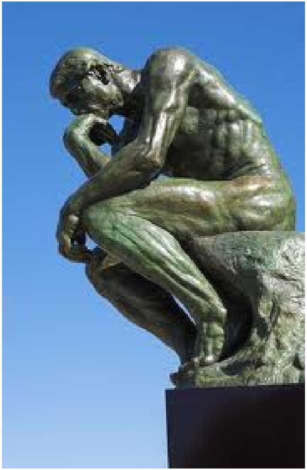

What can we learn from photo reactions?

1. Understanding of the systems at hand.

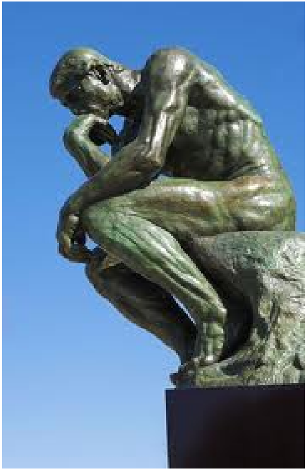

What can we learn from photo reactions?

1. Understanding of the systems at hand.
2. A test of the Hamiltonian at regimes not accessible by elastic reactions.

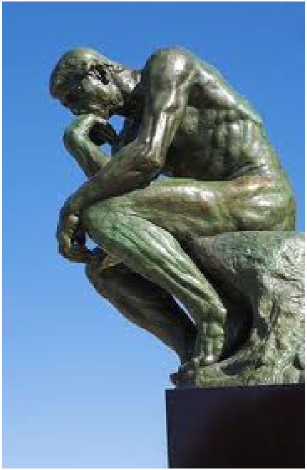

What can we learn from photo reactions?

1. Understanding of the systems at hand.
2. A test of the Hamiltonian at regimes not accessible by elastic reactions.
3. Reaction rates as input for experiments or applications (e.g. astrophysics).

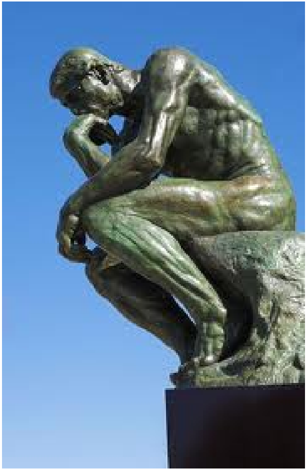

What can we learn from photo reactions?

1. Understanding of the systems at hand.
2. A test of the Hamiltonian at regimes not accessible by elastic reactions.
3. Reaction rates as input for experiments or applications (e.g. astrophysics).
4. Underlying degrees of freedom.

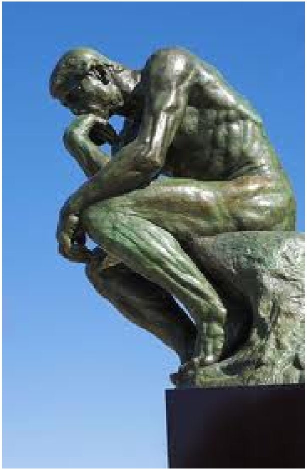

What can we learn from photo reactions?

1. Understanding of the systems at hand.
2. A test of the Hamiltonian at regimes not accessible by elastic reactions.
3. Reaction rates as input for experiments or applications (e.g. astrophysics).
4. Underlying degrees of freedom.
5. The transition from single particle to collective behavior.

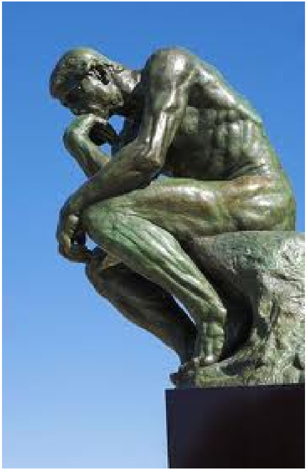

Photo Reactions

The Interaction Hamiltonian between the photon field $\boldsymbol{A}(\boldsymbol{x})$ and the atomic/nuclear system

$$\boxed{H_I = -\frac{e}{c}\int d\boldsymbol{x}\boldsymbol{A}(\boldsymbol{x})\cdot\boldsymbol{J}(\boldsymbol{x})}$$

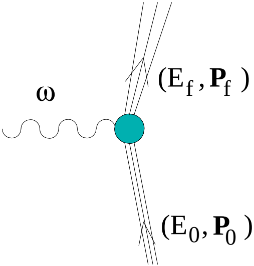

Photo Reactions

The Interaction Hamiltonian between the photon field $\boldsymbol{A}(\boldsymbol{x})$ and the atomic/nuclear system

$$\boxed{H_I = -\frac{e}{c}\int d\boldsymbol{x}\boldsymbol{A}(\boldsymbol{x})\cdot\boldsymbol{J}(\boldsymbol{x})}$$

The current is a sum of convection and spin currents

$$\boxed{\boldsymbol{J}(\boldsymbol{x}) = \boldsymbol{J}_c(\boldsymbol{x}) + \boldsymbol{\nabla}\times\boldsymbol{\mu}(\boldsymbol{x})}$$

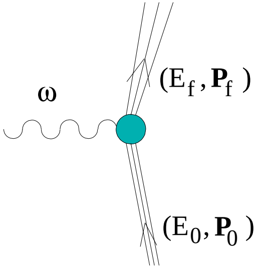

Photo Reactions

The Interaction Hamiltonian between the photon field $\boldsymbol{A}(\boldsymbol{x})$ and the atomic/nuclear system

$$\boxed{H_I = -\frac{e}{c}\int d\boldsymbol{x}\boldsymbol{A}(\boldsymbol{x})\cdot\boldsymbol{J}(\boldsymbol{x})}$$

The current is a sum of convection and spin currents

$$\boxed{\boldsymbol{J}(\boldsymbol{x}) = \boldsymbol{J}_c(\boldsymbol{x}) + \boldsymbol{\nabla}\times\boldsymbol{\mu}(\boldsymbol{x})}$$

$$\boxed{H_I = -\frac{e}{c}\int d\boldsymbol{x}\,\{\boldsymbol{A}(\boldsymbol{x})\cdot\boldsymbol{J}_c(\boldsymbol{x}) + \boldsymbol{B}(\boldsymbol{x})\cdot\boldsymbol{\mu}(\boldsymbol{x})\}}$$

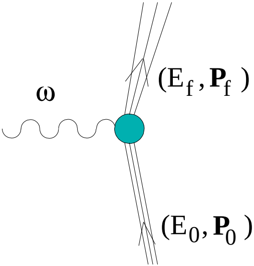

Photo reactions - Theoretical considerations

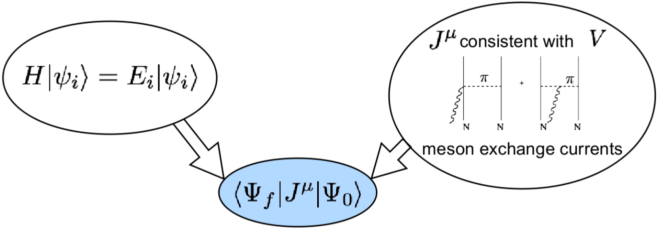

Photo reactions - Theoretical considerations

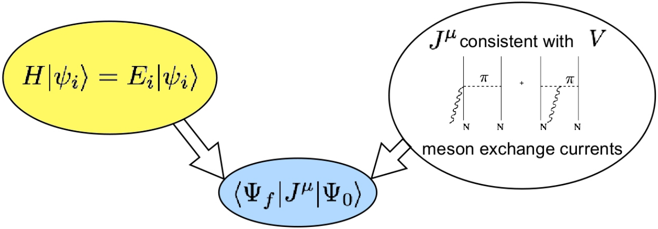

The Wave Functions

- We solve the A-body non-realtivistic Schroedinger equation.
- The Hamiltonian

$$H = T + \sum_{ij} V_{ij}^{(2)} + \sum_{ijk} V_{ijk}^{(3)} + \dots$$

  High precision two-nucleon potentials, well constraint by NN phaseshifts
  Less established 3NF
- EFT provides a solid theoretical framework for construction of the potentials.
- Phenomenological potential models are not that bad either.

Photo reactions - Theoretical considerations (II)

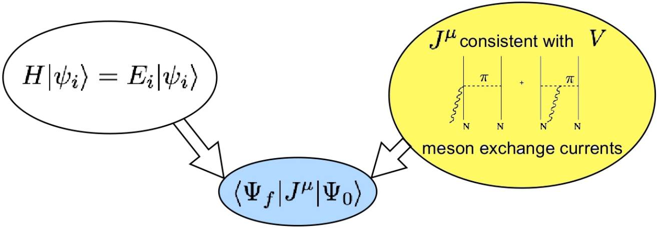

The Electro-Magnetic Current

- The EM current is a sum of convection and spin currents

$$\boxed{\boldsymbol{J}(\boldsymbol{x}) = \boldsymbol{J}_c(\boldsymbol{x}) + \boldsymbol{J}_s(\boldsymbol{x}) = \boldsymbol{J}_c(\boldsymbol{x}) + \nabla \times \boldsymbol{\mu}(\boldsymbol{x})}$$

- Classicaly, the convection current $\boldsymbol{J}_c = \sum_i Z_i \boldsymbol{v}_i$ is the flow of the charged particles.
- In nuclei $\boldsymbol{J}_c(\boldsymbol{x})$ is mainly due to proton movement.
- Meson exchange between nucleons leads to $2, 3, \ldots$-body currents $\boldsymbol{J} = \boldsymbol{J}_1 + \boldsymbol{J}_2 + \ldots$
- Cold atoms are neutral $\boldsymbol{J}_c(\boldsymbol{x}) = 0$ and the current $\boldsymbol{\mu}(\boldsymbol{x})$ is dominated by the electronic spins.

Nuclear Physics - A tale of two potentials

- The nuclear Hamiltonian

$$\boxed{H = -\sum_i \frac{\hbar^2}{2m_N}\nabla_i^2 + \sum_{i<j} V_{ij} + \sum_{i<j<k} V_{ijk} + \ldots}$$

Nuclear Physics - A tale of two potentials

- The nuclear Hamiltonian

$$\boxed{H = -\sum_i \frac{\hbar^2}{2m_N}\nabla_i^2 + \sum_{i<j} V_{ij} + \sum_{i<j<k} V_{ijk} + \dots}$$

- The Potential is composed of EM and NUCLEAR terms.

Nuclear Physics - A tale of two potentials

- The nuclear Hamiltonian

$$\boxed{H = -\sum_i \frac{\hbar^2}{2m_N}\nabla_i^2 + \sum_{i<j} V_{ij} + \sum_{i<j<k} V_{ijk} + \dots}$$

- The Potential is composed of EM and NUCLEAR terms.
- The NUCLEAR force cannot be derived from QCD and must be modeled.

Nuclear Physics - A tale of two potentials

- The nuclear Hamiltonian

$$\boxed{H = -\sum_i \frac{\hbar^2}{2m_N}\nabla_i^2 + \sum_{i<j} V_{ij} + \sum_{i<j<k} V_{ijk} + \dots}$$

- The Potential is composed of EM and NUCLEAR terms.
- The NUCLEAR force cannot be derived from QCD and must be modeled.

The AV18 NN-Force

Nuclear Physics - A tale of two potentials

- The nuclear Hamiltonian

$$\boxed{H = -\sum_i \frac{\hbar^2}{2m_N}\nabla_i^2 + \sum_{i<j} V_{ij} + \sum_{i<j<k} V_{ijk} + \dots}$$

- The Potential is composed of EM and NUCLEAR terms.
- The NUCLEAR force cannot be derived from QCD and must be modeled.

The AV18 NN-Force

- The 2-body potential $V_{ij} = v_{ij}^s + v_{ij}^{2\pi} + v_{ij}^{\pi}$

Nuclear Physics - A tale of two potentials

- The nuclear Hamiltonian

$$\boxed{H = -\sum_i \frac{\hbar^2}{2m_N}\nabla_i^2 + \sum_{i<j} V_{ij} + \sum_{i<j<k} V_{ijk} + \ldots}$$

- The Potential is composed of EM and NUCLEAR terms.
- The NUCLEAR force cannot be derived from QCD and must be modeled.

The AV18 NN-Force

- The 2-body potential $V_{ij} = v_{ij}^s + v_{ij}^{2\pi} + v_{ij}^{\pi}$
- v_{ij}^{π} - A Yukawa type interaction $e^{-\mu r}/r$, $v_{ij}^{2\pi} \propto e^{-2\mu r}/r$.

Nuclear Physics - A tale of two potentials

- The nuclear Hamiltonian

$$\boxed{H = -\sum_i \frac{\hbar^2}{2m_N}\nabla_i^2 + \sum_{i<j} V_{ij} + \sum_{i<j<k} V_{ijk} + \dots}$$

- The Potential is composed of EM and NUCLEAR terms.
- The NUCLEAR force cannot be derived from QCD and must be modeled.

The AV18 NN-Force

- The 2-body potential $V_{ij} = v_{ij}^s + v_{ij}^{2\pi} + v_{ij}^{\pi}$
- v_{ij}^{π} - A Yukawa type interaction $e^{-\mu r}/r$, $v_{ij}^{2\pi} \propto e^{-2\mu r}/r$.
- v_{ij}^s is expanded into a series of operators dictated by the symmetries.

Nuclear Physics - A tale of two potentials

- The nuclear Hamiltonian

$$\boxed{H = -\sum_i \frac{\hbar^2}{2m_N}\nabla_i^2 + \sum_{i<j} V_{ij} + \sum_{i<j<k} V_{ijk} + \ldots}$$

- The Potential is composed of EM and NUCLEAR terms.
- The NUCLEAR force cannot be derived from QCD and must be modeled.

The AV18 NN-Force

- The 2-body potential $V_{ij} = v_{ij}^s + v_{ij}^{2\pi} + v_{ij}^{\pi}$
- v_{ij}^{π} - A Yukawa type interaction $e^{-\mu r}/r$, $v_{ij}^{2\pi} \propto e^{-2\mu r}/r$.
- v_{ij}^s is expanded into a series of operators dictated by the symmetries.
- NNN force must be supplemented to reproduce 3,4-body binding-energies.

Nuclear Physics - A tale of two potentials

- The nuclear Hamiltonian

$$\boxed{H = -\sum_i \frac{\hbar^2}{2m_N}\nabla_i^2 + \sum_{i<j} V_{ij} + \sum_{i<j<k} V_{ijk} + \dots}$$

- The Potential is composed of EM and NUCLEAR terms.
- The NUCLEAR force cannot be derived from QCD and must be modeled.

The AV18 NN-Force

- The 2-body potential $V_{ij} = v_{ij}^s + v_{ij}^{2\pi} + v_{ij}^{\pi}$
- v_{ij}^{π} - A Yukawa type interaction $e^{-\mu r}/r$, $v_{ij}^{2\pi} \propto e^{-2\mu r}/r$.
- v_{ij}^{s} is expanded into a series of operators dictated by the symmetries.
- NNN force must be supplemented to reproduce 3,4-body binding-energies.

The JISP16 Potential

Nuclear Physics - A tale of two potentials

- The nuclear Hamiltonian

$$\boxed{H = -\sum_i \frac{\hbar^2}{2m_N}\nabla_i^2 + \sum_{i<j} V_{ij} + \sum_{i<j<k} V_{ijk} + \ldots}$$

- The Potential is composed of EM and NUCLEAR terms.
- The NUCLEAR force cannot be derived from QCD and must be modeled.

The AV18 NN-Force

- The 2-body potential $V_{ij} = v_{ij}^s + v_{ij}^{2\pi} + v_{ij}^{\pi}$
- v_{ij}^{π} - A Yukawa type interaction $e^{-\mu r}/r$, $v_{ij}^{2\pi} \propto e^{-2\mu r}/r$.
- v_{ij}^s is expanded into a series of operators dictated by the symmetries.
- NNN force must be supplemented to reproduce 3,4-body binding-energies.

The JISP16 Potential

- A formal expansion of the potential

$$V_{ij} = \sum_{lsjnn'} |(ls)jn'\rangle V_{nn'}^{(ls)j} \langle (ls)jn|$$

Nuclear Physics - A tale of two potentials

- The nuclear Hamiltonian

$$\boxed{H = -\sum_i \frac{\hbar^2}{2m_N}\nabla_i^2 + \sum_{i<j} V_{ij} + \sum_{i<j<k} V_{ijk} + \ldots}$$

- The Potential is composed of EM and NUCLEAR terms.
- The NUCLEAR force cannot be derived from QCD and must be modeled.

The AV18 NN-Force

- The 2-body potential $V_{ij} = v_{ij}^s + v_{ij}^{2\pi} + v_{ij}^{\pi}$
- v_{ij}^{π} - A Yukawa type interaction $e^{-\mu r}/r$, $v_{ij}^{2\pi} \propto e^{-2\mu r}/r$.
- v_{ij}^s is expanded into a series of operators dictated by the symmetries.
- NNN force must be supplemented to reproduce 3,4-body binding-energies.

The JISP16 Potential

- A formal expansion of the potential

$$V_{ij} = \sum_{lsjnn'} |(ls)jn'\rangle V_{nn'}^{(ls)j} \langle (ls)jn|$$

- The HO basis is used, $V_{nn'}^{(ls)j}$ fitted to reproduce NN scattering data.

A tale of two potentials

- AV18+UBIX Argonne V18 NN force + Urbana IX NNN force
- JISP16 J-matrix Inverse Scattering Potential, Shirokov *et* al.

Binding Energies

	AV18+UBIX	JISP16	Nature
D	2.24	2.24	2.24
^{3}H	8.48	8.35	8.48
^{3}He	7.74	7.65	7.72
^{4}He	28.5	28.3	28.3

A tale of two potentials

- AV18+UBIX Argonne V18 NN force + Urbana IX NNN force
- JISP16 J-matrix Inverse Scattering Potential, Shirokov *et* al.

Binding Energies

	AV18+UBIX	JISP16	Nature
D	2.24	2.24	2.24
^{3}H	8.48	8.35	8.48
^{3}He	7.74	7.65	7.72
^{4}He	28.5	28.3	28.3

Photodisintegration cross-section for A=2,3,4

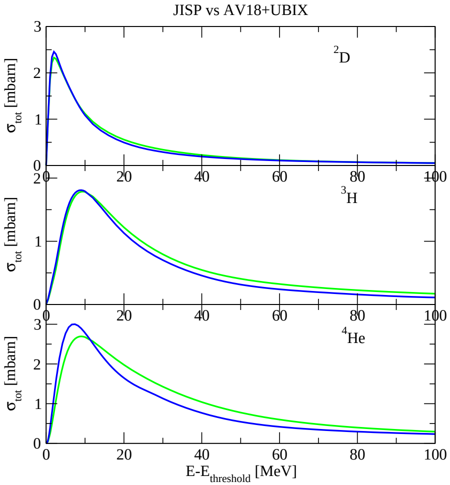

The Experimental Verdict !

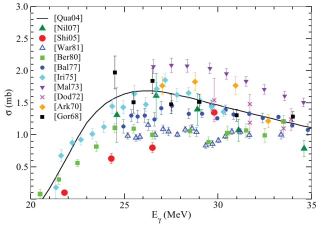

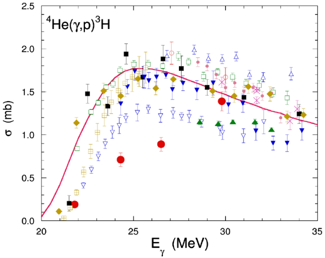

D. Gazit, S. Bacca, N. Barnea, W. Leidemann, and G. Orlandini, PRL **96**, 112301 (2006)
S. Quaglioni, and P. Navratil PLB **652**, 370 (2007)
R. Raut *et* al., PRL **108**, 042502 (2012)
W. Tornow *et* al., PRC**85**, 061001 (2012)

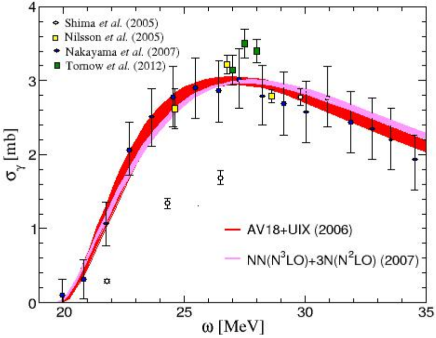

The Experimental Verdict ?

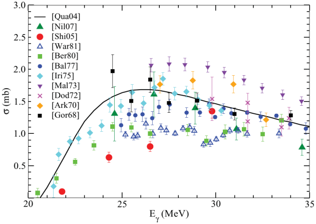

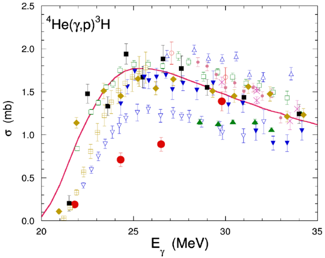

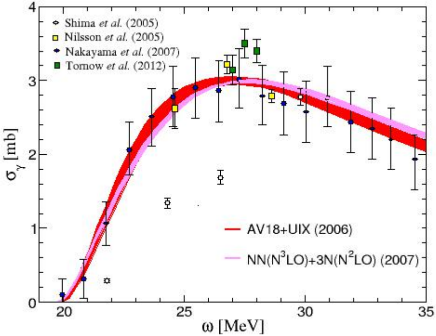

D. Gazit, S. Bacca, N. Barnea, W. Leidemann, and G. Orlandini, PRL **96**, 112301 (2006)
S. Quaglioni, and P. Navratil PLB **652**, 370 (2007)
R. Raut *et* al., PRL **108**, 042502 (2012)
W. Tornow *et* al., PRC**85**, 061001 (2012)

Ultra Cold atoms

- A 3-body bound state $E_3 < 0$ exists even if the 2-body systems is unbound $E_2 > 0$.

Universal insights from few-body land

Chris H. Greene

The ability to tune atomic interactions has inspired theorists and experimentalists to investigate those properties of few-particle systems that hold universally, regardless of the specific nature of the interparticle force.

Physics Today, March 2010

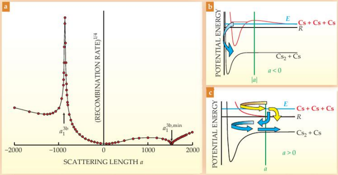

Figure 1. Low-energy recombination of bosonic cesium. **(a)** The numerically calculated recombination rate for $Cs + Cs + Cs \rightarrow Cs_2 + Cs$ plotted as a function of the *Cs–Cs* scattering length *a* measured in Bohr radii. Clearly visible at a negative scattering length is the first Efimov resonance and, at $a = a_1^{3b,min} > 0$, the first destructive interference minimum. The qualitatively different phenomena at large positive and negative *a* follow from the qualitatively different nature of the reaction pathways in those regimes. **(b)** For negative *a*, a system with a small positive energy *E* (blue line) must tunnel over a barrier into the red potential well located at hyperradius $R \ll |a|$. When the scattering length admits a quasi-bound resonance beyond the barrier (horizontal red line), the tunneling rate is enhanced and the system can relax efficiently (blue arrow) to the two-body channel represented by the black potential curve. **(c)** For positive *a*, two distinct paths allow the system to transition to the two-body state at $R \approx a$. In one path (yellow arrows), the system bounces off the red potential barrier and relaxes to the two-body channel while *R* is increasing. In the second pathway (blue arrows), the system transitions to the two-body channel while *R* is decreasing, and then the system rebounds off the black potential barrier. If the scattering length is tuned appropriately, the two paths destructively interfere. (Adapted from ref. 18.)

Ultra Cold atoms

- A 3-body bound state $E_3 < 0$ exists even if the 2-body systems is unbound $E_2 > 0$.
- When $E_2 = 0$, $a_s \longrightarrow \infty$.

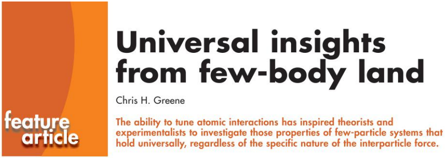
feature article

Universal insights from few-body land

Chris H. Greene

The ability to tune atomic interactions has inspired theorists and experimentalists to investigate those properties of few-particle systems that hold universally, regardless of the specific nature of the interparticle force.

Physics Today, March 2010

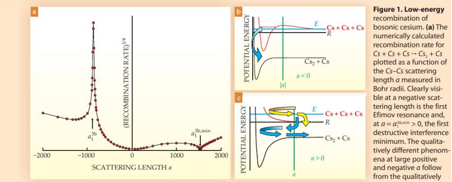

Figure 1. Low-energy recombination of bosonic cesium. **(a)** The numerically calculated recombination rate for $Cs + Cs + Cs \to Cs_2 + Cs$ plotted as a function of the Cs–Cs scattering length a measured in Bohr radii. Clearly visible at a negative scattering length is the first Efimov resonance and, at $a = a_1^{3b,min} > 0$, the first destructive interference minimum. The qualitatively different phenomena at large positive and negative a follow from the qualitatively different nature of the reaction pathways in those regimes. **(b)** For negative a, a system with a small positive energy E (blue line) must tunnel over a barrier into the red potential well located at hyperradius $R \ll |a|$. When the scattering length admits a quasi-bound resonance beyond the barrier (horizontal red line), the tunneling rate is enhanced and the system can relax efficiently (blue arrow) to the two-body channel represented by the black potential curve. **(c)** For positive a, two distinct paths allow the system to transition to the two-body state at $R \approx a$. In one path (yellow arrows), the system bounces off the red potential barrier and relaxes to the two-body channel while R is increasing. In the second pathway (blue arrows), the system transitions to the two-body channel while R is decreasing, and then the system rebounds off the black potential barrier. If the scattering length is tuned appropriately, the two paths destructively interfere. (Adapted from ref. 18.)

Ultra Cold atoms

- A 3-body bound state $E_3 < 0$ exists even if the 2-body systems is unbound $E_2 > 0$.
- When $E_2 = 0$, $a_s \longrightarrow \infty$.
- In 1970 V. Efimov found out that if $E_2 = 0$ the 3-body system will have an **infinite** number of bound states.

Universal insights from few-body land

Chris H. Greene

The ability to tune atomic interactions has inspired theorists and experimentalists to investigate those properties of few-particle systems that hold universally, regardless of the specific nature of the interparticle force.

Physics Today, March 2010

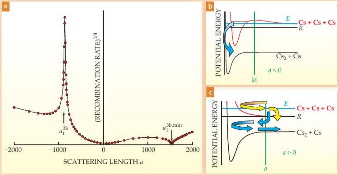

Figure 1. Low-energy recombination of bosonic cesium. **(a)** The numerically calculated recombination rate for $Cs + Cs + Cs \to Cs_2 + Cs$ plotted as a function of the Cs–Cs scattering length a measured in Bohr radii. Clearly visible at a negative scattering length is the first Efimov resonance and, at $a = a_1^{3b,\min} > 0$, the first destructive interference minimum. The qualitatively different phenomena at large positive and negative a follow from the qualitatively different nature of the reaction pathways in those regimes. **(b)** For negative a, a system with a small positive energy E (blue line) must tunnel over a barrier into the red potential well located at hyperradius $R \ll |a|$. When the scattering length admits a quasi-bound resonance beyond the barrier (horizontal red line), the tunneling rate is enhanced and the system can relax efficiently (blue arrow) to the two-body channel represented by the black potential curve. **(c)** For positive a, two distinct paths allow the system to transition to the two-body state at $R \approx a$. In one path (yellow arrows), the system bounces off the red potential barrier and relaxes to the two-body channel while R is increasing. In the second pathway (blue arrows), the system transitions to the two-body channel while R is decreasing, and then the system rebounds off the black potential barrier. If the scattering length is tuned appropriately, the two paths destructively interfere. (Adapted from ref. 18.)

Ultra Cold atoms

- A 3-body bound state $E_3 < 0$ exists even if the 2-body systems is unbound $E_2 > 0$.
- When $E_2 = 0$, $a_s \longrightarrow \infty$.
- In 1970 V. Efimov found out that if $E_2 = 0$ the 3-body system will have an **infinite** number of bound states.
- The 3-body spectrum is $E_n = E_0 e^{-2\pi n/s_0}$ with $s_0 = 1.00623$.

feature article

Universal insights from few-body land

Chris H. Greene

The ability to tune atomic interactions has inspired theorists and experimentalists to investigate those properties of few-particle systems that hold universally, regardless of the specific nature of the interparticle force.

Physics Today, March 2010

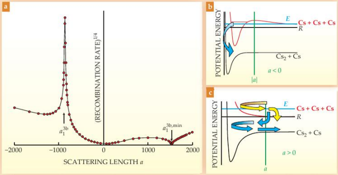

Figure 1. Low-energy recombination of bosonic cesium. **(a)** The numerically calculated recombination rate for $Cs + Cs + Cs \to Cs_2 + Cs$ plotted as a function of the Cs–Cs scattering length a measured in Bohr radii. Clearly visible at a negative scattering length is the first Efimov resonance and, at $a = a_1^{3b,\min} > 0$, the first destructive interference minimum. The qualitatively different phenomena at large positive and negative a follow from the qualitatively different nature of the reaction pathways in those regimes. **(b)** For negative a, a system with a small positive energy E (blue line) must tunnel over a barrier into the red potential well located at hyperradius $R \ll |a|$. When the scattering length admits a quasi-bound resonance beyond the barrier (horizontal red line), the tunneling rate is enhanced and the system can relax efficiently (blue arrow) to the two-body channel represented by the black potential curve. **(c)** For positive a, two distinct paths allow the system to transition to the two-body state at $R \approx a$. In one path (yellow arrows), the system bounces off the red potential barrier and relaxes to the two-body channel while R is increasing. In the second pathway (blue arrows), the system transitions to the two-body channel while R is decreasing, and then the system rebounds off the black potential barrier. If the scattering length is tuned appropriately, the two paths destructively interfere. (Adapted from ref. 18.)

Ultra Cold atoms

- A 3-body bound state $E_3 < 0$ exists even if the 2-body systems is unbound $E_2 > 0$.
- When $E_2 = 0$, $a_s \longrightarrow \infty$.
- In 1970 V. Efimov found out that if $E_2 = 0$ the 3-body system will have an **infinite** number of bound states.
- The 3-body spectrum is $E_n = E_0 e^{-2\pi n/s_0}$ with $s_0 = 1.00623$.
- In atomic traps a_s can be manipulated through the Fesbach resonance.

Universal insights from few-body land

Chris H. Greene

The ability to tune atomic interactions has inspired theorists and experimentalists to investigate those properties of few-particle systems that hold universally, regardless of the specific nature of the interparticle force.

Physics Today, March 2010

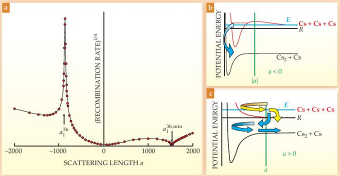

Figure 1. Low-energy recombination of bosonic cesium. **(a)** The numerically calculated recombination rate for $Cs + Cs + Cs \rightarrow Cs_2 + Cs$ plotted as a function of the Cs–Cs scattering length a measured in Bohr radii. Clearly visible at a negative scattering length is the first Efimov resonance and, at $a = a_1^{3b,\mathrm{min}} > 0$, the first destructive interference minimum. The qualitatively different phenomena at large positive and negative a follow from the qualitatively different nature of the reaction pathways in those regimes. **(b)** For negative a, a system with a small positive energy E (blue line) must tunnel over a barrier into the red potential well located at hyperradius $R \ll |a|$. When the scattering length admits a quasi-bound resonance beyond the barrier (horizontal red line), the tunneling rate is enhanced and the system can relax efficiently (blue arrow) to the two-body channel represented by the black potential curve. **(c)** For positive a, two distinct paths allow the system to transition to the two-body state at $R \approx a$. In one path (yellow arrows), the system bounces off the red potential barrier and relaxes to the two-body channel while R is increasing. In the second pathway (blue arrows), the system transitions to the two-body channel while R is decreasing, and then the system rebounds off the black potential barrier. If the scattering length is tuned appropriately, the two paths destructively interfere. (Adapted from ref. 18.)

Ultra Cold atoms

- A 3-body bound state $E_3 < 0$ exists even if the 2-body systems is unbound $E_2 > 0$.
- When $E_2 = 0$, $a_s \longrightarrow \infty$.
- In 1970 V. Efimov found out that if $E_2 = 0$ the 3-body system will have an **infinite** number of bound states.
- The 3-body spectrum is $E_n = E_0 e^{-2\pi n/s_0}$ with $s_0 = 1.00623$.
- In atomic traps a_s can be manipulated through the Fesbach resonance.
- Particle losses in traps are closely related to Efimov's physics through the 3-body recombination process

$$A + A + A \longrightarrow A_2 + A$$

Universal insights from few-body land

Chris H. Greene

The ability to tune atomic interactions has inspired theorists and experimentalists to investigate those properties of few-particle systems that hold universally, regardless of the specific nature of the interparticle force.

Physics Today, March 2010

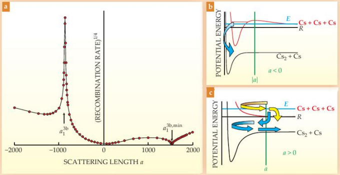

Figure 1. Low-energy recombination of bosonic cesium. **(a)** The numerically calculated recombination rate for $Cs + Cs + Cs \rightarrow Cs_2 + Cs$ plotted as a function of the Cs–Cs scattering length a measured in Bohr radii. Clearly visible at a negative scattering length is the first Efimov resonance and, at $a = a_1^{3b,\min} > 0$, the first destructive interference minimum. The qualitatively different phenomena at large positive and negative a follow from the qualitatively different nature of the reaction pathways in those regimes. **(b)** For negative a, a system with a small positive energy E (blue line) must tunnel over a barrier into the red potential well located at hyperradius $R \ll |a|$. When the scattering length admits a quasi-bound resonance beyond the barrier (horizontal red line), the tunneling rate is enhanced and the system can relax efficiently (blue arrow) to the two-body channel represented by the black potential curve. **(c)** For positive a, two distinct paths allow the system to transition to the two-body state at $R \approx a$. In one path (yellow arrows), the system bounces off the red potential barrier and relaxes to the two-body channel while R is increasing. In the second pathway (blue arrows), the system transitions to the two-body channel while R is decreasing, and then the system rebounds off the black potential barrier. If the scattering length is tuned appropriately, the two paths destructively interfere. (Adapted from ref. 18.)

Few-Body Universality in a Bosonic ^{7}Li system

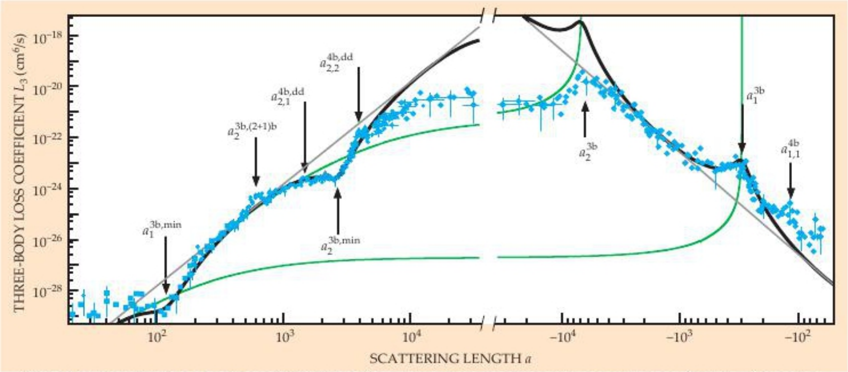

Photoassociation of Atomic Molecules

RF-induce atom loss resonaces for different values of bias magnetic fields.

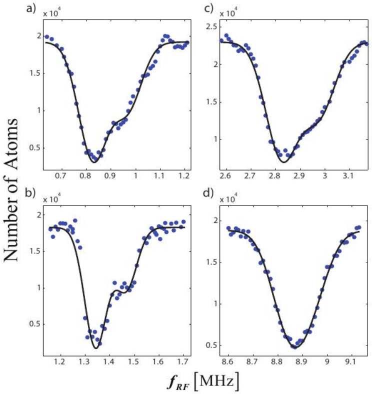

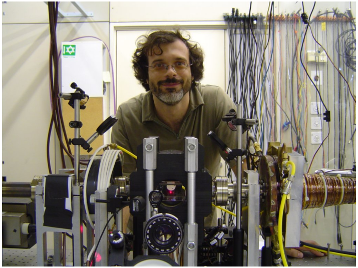

O. Machtey, Z. Shotan, N. Gross and L. Khaykovich
PRL **108**, 210406 (2012)

The Static Response - Inelastic Reactions

- The response of an A-particle system is closely related to the static moments of the charge density

$$\rho(\boldsymbol{x}) = \sum_{i}^{A} Z_i \delta(\boldsymbol{x} - \boldsymbol{r}_i)$$

The Static Response - Inelastic Reactions

- The response of an A-particle system is closely related to the static moments of the charge density

$$\rho(\boldsymbol{x}) = \sum_i^A Z_i \delta(\boldsymbol{x} - \boldsymbol{r}_i)$$

- The Fourier Transform

$$\rho(\boldsymbol{q}) = \int d\boldsymbol{x} \rho(\boldsymbol{x}) e^{i\boldsymbol{q}\cdot\boldsymbol{x}} = \sum_i^A Z_i e^{i\boldsymbol{q}\cdot\boldsymbol{r}_i}$$

The Static Response - Inelastic Reactions

- The response of an A-particle system is closely related to the static moments of the charge density

$$\rho(\boldsymbol{x}) = \sum_{i}^{A} Z_i \delta(\boldsymbol{x} - \boldsymbol{r}_i)$$

- The Fourier Transform

$$\rho(\boldsymbol{q}) = \int d\boldsymbol{x} \rho(\boldsymbol{x}) e^{i\boldsymbol{q}\cdot\boldsymbol{x}} = \sum_{i}^{A} Z_i e^{i\boldsymbol{q}\cdot\boldsymbol{r}_i}$$

- In the long wavelength limit $q \longrightarrow 0$

$$\rho(\boldsymbol{q}) \approx \sum_{i}^{A} Z_i + i \sum_{i}^{A} Z_i \boldsymbol{q}\cdot\boldsymbol{r}_i - \frac{1}{2}\sum_{i}^{A} Z_i (\boldsymbol{q}\cdot\boldsymbol{r}_i)^2$$

The Static Response - Inelastic Reactions

- The response of an A-particle system is closely related to the static moments of the charge density

$$\rho(\boldsymbol{x}) = \sum_i^A Z_i \delta(\boldsymbol{x} - \boldsymbol{r}_i)$$

- The Fourier Transform

$$\rho(\boldsymbol{q}) = \int d\boldsymbol{x} \rho(\boldsymbol{x}) e^{i\boldsymbol{q}\cdot\boldsymbol{x}} = \sum_i^A Z_i e^{i\boldsymbol{q}\cdot\boldsymbol{r}_i}$$

- In the long wavelength limit $q \longrightarrow 0$

$$\rho(\boldsymbol{q}) \approx \sum_i^A Z_i + i \sum_i^A Z_i \boldsymbol{q}\cdot\boldsymbol{r}_i - \frac{1}{2}\sum_i^A Z_i (\boldsymbol{q}\cdot\boldsymbol{r}_i)^2$$

- For a system of **identical** particles

$$\rho(\boldsymbol{q}) \approx AZ_1 + iZ_1 \boldsymbol{R}_{cm} - \frac{1}{2} Z_1 \sum_i^A \big(\frac{q^2 r_i^2}{6} + 4\pi \frac{q^2 r_i^2}{15} \sum_m Y_{2-m}(\hat{q}) Y_{2m}(\hat{r}_i) \big)$$

The Static Response - Inelastic Reactions

- The response of an A-particle system is closely related to the static moments of the charge density

$$\rho(\boldsymbol{x}) = \sum_{i}^{A} Z_i \delta(\boldsymbol{x} - \boldsymbol{r}_i)$$

- The Fourier Transform

$$\rho(\boldsymbol{q}) = \int d\boldsymbol{x} \rho(\boldsymbol{x}) e^{i\boldsymbol{q}\cdot\boldsymbol{x}} = \sum_{i}^{A} Z_i e^{i\boldsymbol{q}\cdot\boldsymbol{r}_i}$$

- In the long wavelength limit $q \longrightarrow 0$

$$\rho(\boldsymbol{q}) \approx \sum_{i}^{A} Z_i + i\sum_{i}^{A} Z_i \boldsymbol{q}\cdot\boldsymbol{r}_i - \frac{1}{2}\sum_{i}^{A} Z_i (\boldsymbol{q}\cdot\boldsymbol{r}_i)^2$$

- For a system of **identical** particles

$$\rho(\boldsymbol{q}) \approx AZ_1 + iZ_1 \boldsymbol{R}_{cm} - \frac{1}{2} Z_1 \sum_{i}^{A} \Big(\frac{q^2 r_i^2}{6} + 4\pi \frac{q^2 r_i^2}{15} \sum_{m} Y_{2-m}(\hat{q}) Y_{2m}(\hat{r}_i) \Big)$$

- **Conclusion A:** In general the Dipole is the leading term.

The Static Response - Inelastic Reactions

- The response of an A-particle system is closely related to the static moments of the charge density

$$\rho(\boldsymbol{x}) = \sum_i^A Z_i \delta(\boldsymbol{x} - \boldsymbol{r}_i)$$

- The Fourier Transform

$$\rho(\boldsymbol{q}) = \int d\boldsymbol{x} \rho(\boldsymbol{x}) e^{i\boldsymbol{q}\cdot\boldsymbol{x}} = \sum_i^A Z_i e^{i\boldsymbol{q}\cdot\boldsymbol{r}_i}$$

- In the long wavelength limit $q \longrightarrow 0$

$$\rho(\boldsymbol{q}) \approx \sum_i^A Z_i + i\sum_i^A Z_i \boldsymbol{q}\cdot\boldsymbol{r}_i - \frac{1}{2}\sum_i^A Z_i (\boldsymbol{q}\cdot\boldsymbol{r}_i)^2$$

- For a system of **identical** particles

$$\rho(\boldsymbol{q}) \approx AZ_1 + iZ_1\boldsymbol{R}_{cm} - \frac{1}{2}Z_1\sum_i^A \left(\frac{q^2 r_i^2}{6} + 4\pi\frac{q^2 r_i^2}{15}\sum_m Y_{2-m}(\hat{q})Y_{2m}(\hat{r}_i)\right)$$

- **Conclusion A:** In general the Dipole is the leading term.
- **Conclusion B:** For identical particles the leading terms are $\hat{R}^2$ and $\hat{Q}$.

Photo Reactions with Cold-Atoms

- For RF photons in the MHz region the wave length is meters so $qR \ll 1$.

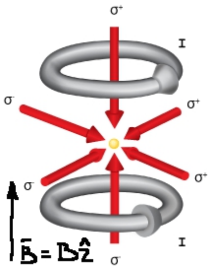

Photo Reactions with Cold-Atoms

- For RF photons in the MHz region the wave length is meters so $qR \ll 1$.
- The Atoms reside in a strong magnetic field, thus spins are “frozen”

$$|\Psi_0\rangle = \Phi_0(\boldsymbol{r}_i)|m_F^1 m_F^2 \ldots m_F^A\rangle$$

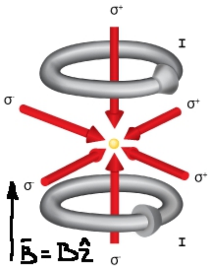

Photo Reactions with Cold-Atoms

- For RF photons in the MHz region the wave length is meters so $qR \ll 1$.
- The Atoms reside in a strong magnetic field, thus spins are "frozen"

$$|\Psi_0\rangle = \Phi_0(\boldsymbol{r}_i)|m_F^1 m_F^2 \ldots m_F^A\rangle$$

- In the final state the photon can either change one of the spins or leave them untouched.

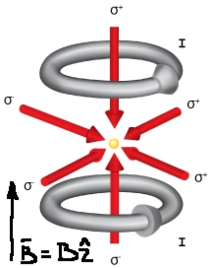

Photo Reactions with Cold-Atoms

- For RF photons in the MHz region the wave length is meters so $qR \ll 1$.
- The Atoms reside in a strong magnetic field, thus spins are “frozen”

$$|\Psi_0\rangle = \Phi_0(\boldsymbol{r}_i)|m_F^1 m_F^2 \dots m_F^A\rangle$$

- In the final state the photon can either change one of the spins or leave them untouched.
- Spin-flip reaction

$$\boxed{|m_F^1 m_F^2 \dots m_F^A\rangle \longrightarrow |m_F^1 m_F^2 \pm 1 \dots m_F^A\rangle}$$

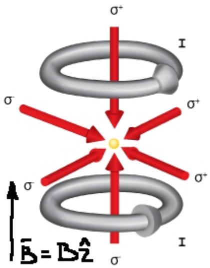

Photo Reactions with Cold-Atoms

- For RF photons in the MHz region the wave length is meters so $qR \ll 1$.
- The Atoms reside in a strong magnetic field, thus spins are "frozen"

$$|\Psi_0\rangle = \Phi_0(\boldsymbol{r}_i)|m_F^1 m_F^2 \ldots m_F^A\rangle$$

- In the final state the photon can either change one of the spins or leave them untouched.
- Spin-flip reaction

$$\boxed{|m_F^1 m_F^2 \ldots m_F^A\rangle \longrightarrow |m_F^1 m_F^2 \pm 1 \ldots m_F^A\rangle}$$

- Frozen-Spin reaction

$$\boxed{|m_F^1 m_F^2 \ldots m_F^A\rangle \longrightarrow |m_F^1 m_F^2 \ldots m_F^A\rangle}$$

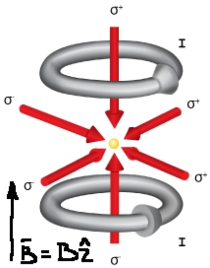

Photo Reactions with Cold-Atoms

- For Spin-flip reactions we get the "Fermi" operator

$$\boxed{R(\omega) = Ck \sum_{f,\lambda} \left|\langle \Phi_f | \Phi_0 \rangle\right|^2 \delta(E_f - E_0 - \omega)}$$

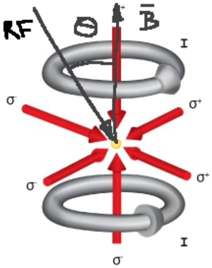

Photo Reactions with Cold-Atoms

- For Spin-flip reactions we get the "Fermi" operator

$$\boxed{R(\omega) = Ck \sum_{f,\lambda} \left|\langle \Phi_f | \Phi_0 \rangle\right|^2 \delta(E_f - E_0 - \omega)}$$

- For Frozen-Spin reactions we get a sum of the monopole operator $\hat{M} = R^2 = \sum r_i^2$ and the Quadrupole operator $\hat{Q} = \sum r_i^2 Y_2(\hat{r}_i)$

$$\boxed{\boldsymbol{O} = \alpha \hat{M} + \beta \hat{Q}}$$

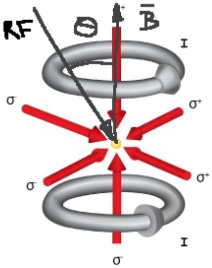

Photo Reactions with Cold-Atoms

- For Spin-flip reactions we get the "Fermi" operator

$$\boxed{R(\omega) = Ck \sum_{f,\lambda} \left| \langle \Phi_f | \Phi_0 \rangle \right|^2 \delta(E_f - E_0 - \omega)}$$

- For Frozen-Spin reactions we get a sum of the monopole operator $\hat{M} = R^2 = \sum r_i^2$ and the Quadrupole operator $\hat{Q} = \sum r_i^2 Y_2(\hat{r}_i)$

$$\boxed{\boldsymbol{O} = \alpha \hat{M} + \beta \hat{Q}}$$

- The response is given by

$$\boxed{R(\omega) = k^5 \sum_{f,\lambda} \left| \langle \Phi_f | \boldsymbol{O} | \Phi_0 \rangle \right|^2 \delta(E_f - E_0 - \omega)}$$

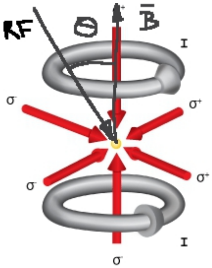

Photoassociation of The Atomic Dimer

- For the dimer case the response function can be written as

$$\boxed{R(\omega) = C\omega^5 \left[\frac{1}{6^2}|\langle\varphi_0(q)\|\hat{M}\|\psi_0\rangle|^2 + \frac{1}{5\cdot 15^2}|\langle\varphi_2(q)\|\hat{Q}\|\psi_0\rangle|^2\right]}$$

Photoassociation of The Atomic Dimer

- For the dimer case the response function can be written as

$$\boxed{R(\omega) = C\omega^5 \left[\frac{1}{6^2} |\langle \varphi_0(q) \| \hat{M} \| \psi_0 \rangle|^2 + \frac{1}{5 \cdot 15^2} |\langle \varphi_2(q) \| \hat{Q} \| \psi_0 \rangle|^2 \right]}$$

- Where the G.S. wave function is given by

$$\psi_0 = Y_0 \sqrt{2\kappa} e^{-\kappa r}/r \quad ; \quad \kappa \approx 1/a_s$$

Photoassociation of The Atomic Dimer

- For the dimer case the response function can be written as

$$\boxed{R(\omega) = C\omega^5 \left[\frac{1}{6^2} |\langle \varphi_0(q) \| \hat{M} \| \psi_0 \rangle|^2 + \frac{1}{5 \cdot 15^2} |\langle \varphi_2(q) \| \hat{Q} \| \psi_0 \rangle|^2 \right]}$$

- Where the G.S. wave function is given by

$$\psi_0 = Y_0 \sqrt{2\kappa} e^{-\kappa r}/r \quad ; \quad \kappa \approx 1/a_s$$

- The continuum state is given by $\varphi_\ell(q) = Y_\ell(\hat{r})\chi_\ell(r)/r$

$$\chi_\ell(r) = 2qr[\cos\delta_\ell j_\ell(qr) - \sin\delta_\ell n_\ell(qr)]$$

Photoassociation of The Atomic Dimer

- For the dimer case the response function can be written as

$$\boxed{R(\omega) = C\omega^5 \left[\frac{1}{6^2} |\langle \varphi_0(q) \| \hat{M} \| \psi_0 \rangle|^2 + \frac{1}{5 \cdot 15^2} |\langle \varphi_2(q) \| \hat{Q} \| \psi_0 \rangle|^2 \right]}$$

- Where the G.S. wave function is given by

$$\psi_0 = Y_0 \sqrt{2\kappa} e^{-\kappa r}/r \quad ; \quad \kappa \approx 1/a_s$$

- The continuum state is given by $\varphi_\ell(q) = Y_\ell(\hat{r}) \chi_\ell(r)/r$

$$\chi_\ell(r) = 2qr[\cos \delta_\ell j_\ell(qr) - \sin \delta_\ell n_\ell(qr)]$$

- The $\ell = 0$ matrix element

$$\boxed{|\langle \varphi_0(q) \| \hat{M} \| \psi_0 \rangle|^2 = \frac{1}{4\pi} \left(\frac{4q\sqrt{2\kappa}}{(q^2 + \kappa^2)^3} \right)^2 \left[\cos \delta_0 (3\kappa^2 - q^2) - \sin \delta_0 \frac{\kappa}{q} (3q^2 - \kappa^2) \right]^2}$$

Photoassociation of The Atomic Dimer

- For the dimer case the response function can be written as

$$\boxed{R(\omega) = C\omega^5 \left[\frac{1}{6^2} |\langle \varphi_0(q) \| \hat{M} \| \psi_0 \rangle|^2 + \frac{1}{5 \cdot 15^2} |\langle \varphi_2(q) \| \hat{Q} \| \psi_0 \rangle|^2 \right]}$$

- Where the G.S. wave function is given by

$$\psi_0 = Y_0 \sqrt{2\kappa} e^{-\kappa r}/r \quad ; \quad \kappa \approx 1/a_s$$

- The continuum state is given by $\varphi_\ell(q) = Y_\ell(\hat{r})\chi_\ell(r)/r$

$$\chi_\ell(r) = 2qr[\cos\delta_\ell j_\ell(qr) - \sin\delta_\ell n_\ell(qr)]$$

- The $\ell = 0$ matrix element

$$\boxed{|\langle \varphi_0(q) \| \hat{M} \| \psi_0 \rangle|^2 = \frac{1}{4\pi} \left(\frac{4q\sqrt{2\kappa}}{(q^2+\kappa^2)^3} \right)^2 \left[\cos\delta_0 (3\kappa^2 - q^2) - \sin\delta_0 \frac{\kappa}{q}(3q^2 - \kappa^2) \right]^2}$$

- The $\ell = 2$ matrix element, assuming $\delta_2 = 0$

$$\boxed{|\langle \varphi_2(q) \| \hat{Q} \| \psi_0 \rangle|^2 = \frac{5}{4\pi} \left[\frac{16q^3\sqrt{2\kappa}}{(q^2+\kappa^2)^3} \right]^2}$$

Photoassociation of The Atomic Dimer

The s-wave and d-wave components in the response function

- upper panel $a/r_{eff} = 2$
- lower pannel $a/r_{eff} = 200$
- red - r^2 monopole
- blue - quadrupole

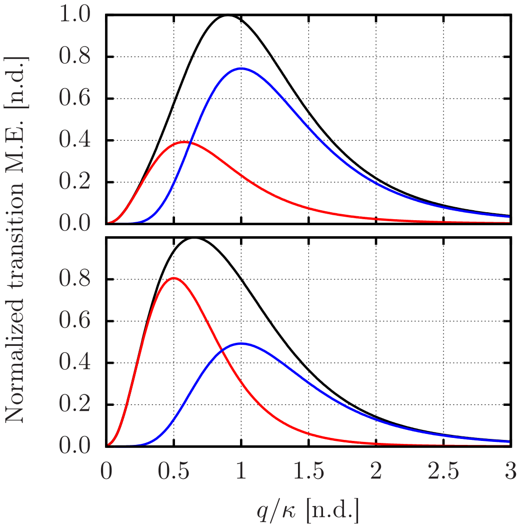

Photoassociation rates

Photoassociation of ^{7}Li atoms

$a_s = 1000\mathrm{a}_0$
$T = 5\mu\mathrm{K}$ (lower panel), $T = 25\mu\mathrm{K}$ (upper panel)

red - r^2 monopole, blue - quadrupole

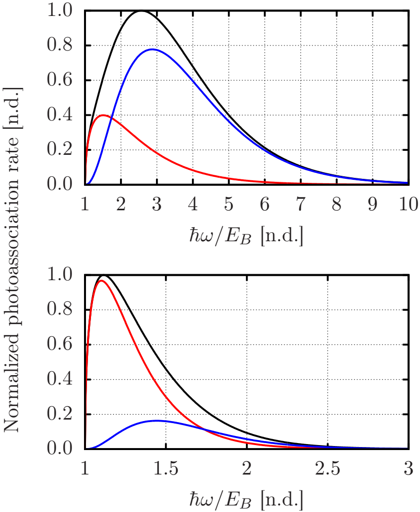

Photoassociation rates

Photoassociation of ^{7}Li atoms

$a_s = 1000\mathrm{a}_0$
$T = 5\mu$K (lower panel), $T = 25\mu$K (upper panel)

red - r^2 monopole, blue - quadrupole

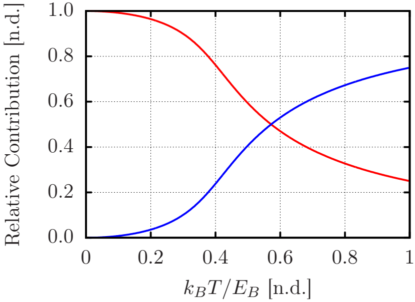

The relative contribution to the peak

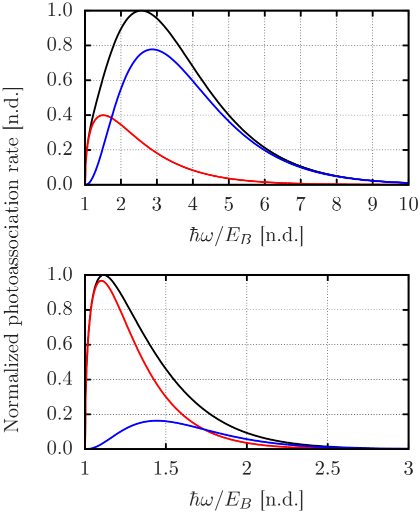

Photoassociation of The Atomic Dimer

Comparison to the Khaykovich group data

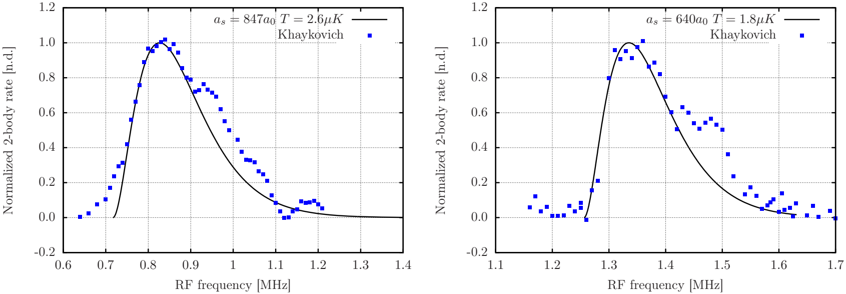

- The fitted values of a_s and T are in reasonable agreement with the estimates of the experimental group.
- Effect of RF field on dimers not included.
- Finite time effect
- Disagreement are due to 3-body (4-body?) association.
- Effects of $\delta_2 \neq 0$ are negligible.

The Atomic Trimer

The quadrupole response of the bosonic trimer

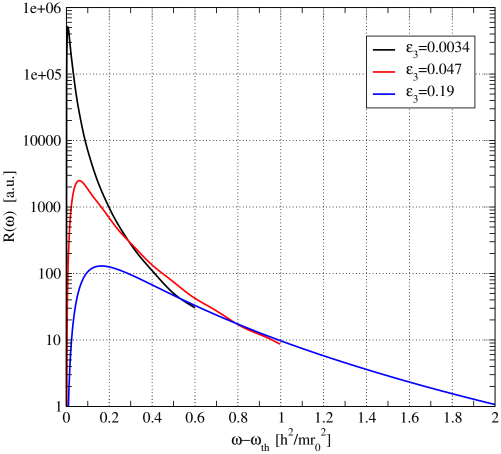

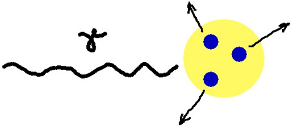

E. Liverts, B. Bazak, and N. Barnea
Phys. Rev. Lett. **108**, 112501 (2012).

Photodisintegration Sum Rules

$$\boxed{S_n \equiv \int_{\omega_{th}}^{\infty} d\omega\, \omega^n\, R(\omega)}$$

Photodisintegration Sum Rules

$$\boxed{S_n \equiv \int_{\omega_{th}}^{\infty} d\omega\, \omega^n\, R(\omega)}$$

The sum rule S_n

- Exists if $R(\omega) \longrightarrow 0$ faster than ω^{-n-1}.
- Can be expressed as GS observable utilizing the closure of the eigenstates of H.

Photodisintegration Sum Rules

$$\boxed{S_n \equiv \int_{\omega_{th}}^{\infty} d\omega\, \omega^n\, R(\omega)}$$

The sum rule S_n

- Exists if $R(\omega) \longrightarrow 0$ faster than ω^{-n-1}.
- Can be expressed as GS observable utilizing the closure of the eigenstates of H.

$$\begin{aligned}
S_1 &= \langle 0 | \left[\mathbf{O}, [H, \mathbf{O}]\right] | 0 \rangle = \langle 0 | \mathbf{O}\,(H - E_0)\,\mathbf{O} | 0 \rangle \\
S_0 &= \langle 0 | \mathbf{O}\mathbf{O} | 0 \rangle \\
S_{-1} &= \langle 0 | \mathbf{O} \frac{1}{H - E_0} \mathbf{O} | 0 \rangle
\end{aligned}$$

Naive Scaling

- Using simple dimensional arguments we expect that

$$r \sim 1/\sqrt{E}$$

- The Quadrupole operator behaves as r^2 so

$$R(\omega) \sim r^4/E \sim 1/E^3$$

- It follows that the sum rules should fulfill

$$S_n \sim 1/E^{2-n}$$

- or

$$S_0 \sim 1/E^2$$
$$S_{-1} \sim 1/E^3$$
$$S_0/S_{-1} \sim E$$

Calculated Sum Rules

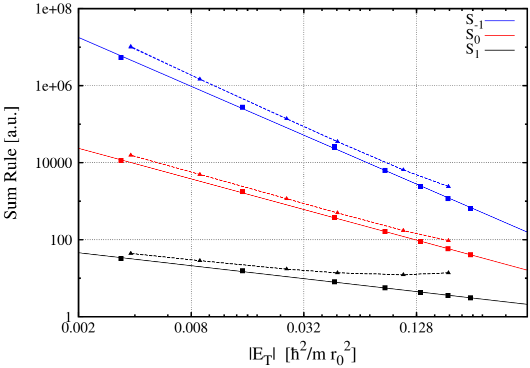

- Squares Gauss Potential
- Triangles Yukawa Potential

Fitted lines

$$S_{-1} = A_{-1} E^{-2.13}$$

$$S_0 = A_0 E^{-1.34}$$

$$S_1 = A_1 E^{-0.55}$$

Naive scaling doesn't work !!!

A For S_1 we got a power of 0.55 instead of 1.

B For S_0 we got a power of 1.33 instead of 2.

C For S_{-1} we got a power of 2.13 instead of 3.

D The ration $S_n/S_{n-1} \sim E^{0.8}$ instead of $S_n/S_{n-1} \sim E$.

E The results seems to be independent of the short range specifications of the potential.

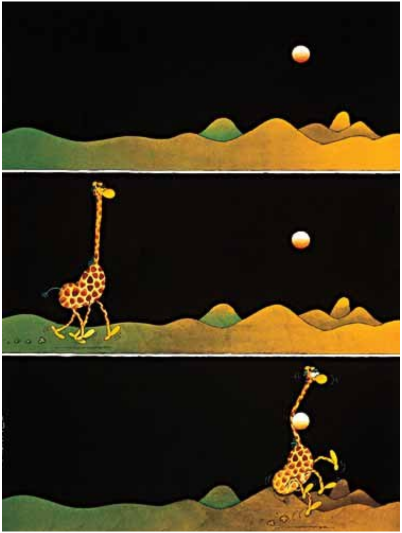

Summary and Conclusions

1. The new RF experiments in Cold-Atoms systems carry much in common with photo-reactions and charged current reactions in nuclei.

Summary and Conclusions

1. The new RF experiments in Cold-Atoms systems carry much in common with photo-reactions and charged current reactions in nuclei.
2. For spin-flip reaction a Fermi type operator is the leading contribution to the cross-section, and $R(\omega) \propto \omega$.

Summary and Conclusions

1. The new RF experiments in Cold-Atoms systems carry much in common with photo-reactions and charged current reactions in nuclei.
2. For spin-flip reaction a Fermi type operator is the leading contribution to the cross-section, and $R(\omega) \propto \omega$.
3. For frozen-spin reactions the monopole R^2 and the Quadrupole are the leading terms, and $R(\omega) \propto \omega^5$.

Summary and Conclusions

1. The new RF experiments in Cold-Atoms systems carry much in common with photo-reactions and charged current reactions in nuclei.
2. For spin-flip reaction a Fermi type operator is the leading contribution to the cross-section, and $R(\omega) \propto \omega$.
3. For frozen-spin reactions the monopole R^2 and the Quadrupole are the leading terms, and $R(\omega) \propto \omega^5$.
4. We have studied Dimer formation and found that the reaction mechanism change from monopole to quadrupole with increasing gas temprature.

Summary and Conclusions

1. The new RF experiments in Cold-Atoms systems carry much in common with photo-reactions and charged current reactions in nuclei.
2. For spin-flip reaction a Fermi type operator is the leading contribution to the cross-section, and $R(\omega) \propto \omega$.
3. For frozen-spin reactions the monopole R^2 and the Quadrupole are the leading terms, and $R(\omega) \propto \omega^5$.
4. We have studied Dimer formation and found that the reaction mechanism change from monopole to quadrupole with increasing gas temprature.
5. We have studied the Quadrupole response of a bosonic trimer near threshold.

Summary and Conclusions

1. The new RF experiments in Cold-Atoms systems carry much in common with photo-reactions and charged current reactions in nuclei.
2. For spin-flip reaction a Fermi type operator is the leading contribution to the cross-section, and $R(\omega) \propto \omega$.
3. For frozen-spin reactions the monopole R^2 and the Quadrupole are the leading terms, and $R(\omega) \propto \omega^5$.
4. We have studied Dimer formation and found that the reaction mechanism change from monopole to quadrupole with increasing gas temprature.
5. We have studied the Quadrupole response of a bosonic trimer near threshold.
6. We have seen that the response function diverge as $E_3 \longrightarrow 0$.

Summary and Conclusions

1. The new RF experiments in Cold-Atoms systems carry much in common with photo-reactions and charged current reactions in nuclei.
2. For spin-flip reaction a Fermi type operator is the leading contribution to the cross-section, and $R(\omega) \propto \omega$.
3. For frozen-spin reactions the monopole R^2 and the Quadrupole are the leading terms, and $R(\omega) \propto \omega^5$.
4. We have studied Dimer formation and found that the reaction mechanism change from monopole to quadrupole with increasing gas temprature.
5. We have studied the Quadrupole response of a bosonic trimer near threshold.
6. We have seen that the response function diverge as $E_3 \longrightarrow 0$.
7. The sum-rules S_1, S_0, S_{-1} diverge as well.

Summary and Conclusions

1. The new RF experiments in Cold-Atoms systems carry much in common with photo-reactions and charged current reactions in nuclei.
2. For spin-flip reaction a Fermi type operator is the leading contribution to the cross-section, and $R(\omega) \propto \omega$.
3. For frozen-spin reactions the monopole R^2 and the Quadrupole are the leading terms, and $R(\omega) \propto \omega^5$.
4. We have studied Dimer formation and found that the reaction mechanism change from monopole to quadrupole with increasing gas temprature.
5. We have studied the Quadrupole response of a bosonic trimer near threshold.
6. We have seen that the response function diverge as $E_3 \longrightarrow 0$.
7. The sum-rules S_1, S_0, S_{-1} diverge as well.
8. We note that the divergence pattern of the sum-rules doesn't follow the simple dimensional analysis.

Summary and Conclusions

1. The new RF experiments in Cold-Atoms systems carry much in common with photo-reactions and charged current reactions in nuclei.
2. For spin-flip reaction a Fermi type operator is the leading contribution to the cross-section, and $R(\omega) \propto \omega$.
3. For frozen-spin reactions the monopole R^2 and the Quadrupole are the leading terms, and $R(\omega) \propto \omega^5$.
4. We have studied Dimer formation and found that the reaction mechanism change from monopole to quadrupole with increasing gas temprature.
5. We have studied the Quadrupole response of a bosonic trimer near threshold.
6. We have seen that the response function diverge as $E_3 \longrightarrow 0$.
7. The sum-rules S_1, S_0, S_{-1} diverge as well.
8. We note that the divergence pattern of the sum-rules doesn't follow the simple dimensional analysis.

Summary and Conclusions

1. The new RF experiments in Cold-Atoms systems carry much in common with photo-reactions and charged current reactions in nuclei.
2. For spin-flip reaction a Fermi type operator is the leading contribution to the cross-section, and $R(\omega) \propto \omega$.
3. For frozen-spin reactions the monopole R^2 and the Quadrupole are the leading terms, and $R(\omega) \propto \omega^5$.
4. We have studied Dimer formation and found that the reaction mechanism change from monopole to quadrupole with increasing gas temprature.
5. We have studied the Quadrupole response of a bosonic trimer near threshold.
6. We have seen that the response function diverge as $E_3 \longrightarrow 0$.
7. The sum-rules S_1, S_0, S_{-1} diverge as well.
8. We note that the divergence pattern of the sum-rules doesn't follow the simple dimensional analysis.

HAPPY NEW YEAR 5773